Heat Conduction Analysis of Nano-Tip in Thermal-assisted Data Storage using Molecular Dynamics Simulation

X. J. Liu[a,b], J. P. Yang[b] and Y. W. Yang[c]

[a] Nanyang Technological University, Nanyang Avenue, Singapore 639798, liux0014@ntu.edu.sg
[b] Data Storage Institute, DSI Building, 5 Engineering Drive 1, Singapore 117608, Yang_Jiaping@dsi.a-star.edu.sg
[c] Nanyang Technological University, Nanyang Avenue, Singapore 639798, cywyang@ntu.edu.sg

ABSTRACT

In the thermal-assisted data storage technologies, the behavior of heat transfer in nano-tip during thermo-mechanical data bit formation process is a critical factor affecting the areal storage density, data bit writing/reading speed and system reliability. In this paper, the thermal properties of a nano-tip are analyzed using the nonequilibrium molecular dynamics simulation, which is based on the Tersoff-type three-body potential and the Gear's five-value predictor-corrector integration algorithm. For comparison, a nano-cube is also simulated. The simulated results show that the effects of the nano-structural configuration and boundary conditions on the thermal transport are remarkable, which can be attributed to the phonon boundary-scattering and possible phonon spectrum modification. Finally, the thermal conductivities of the nano-tip and the nano-cube are calculated.

Keywords: nano-tip, molecular dynamics simulation, thermal conductivity, data storage

1 INTRODUCTION

Within a few years, magnetic storage technology is meeting a fundamental challenge, the well-known superparamagnetic limit. In order to propel data storage industry to continuously develop new storage technologies for large storage capacity and high data transfer rate, several attractive alternate proposals have been put forward, such as the heat-assisted magnetic recording (HARM) technology [1] and the scanning probe-based data storage technology [2, 3, 4]. In these recording technologies, the behavior of heat transfer in the nano-tips as well as between the nano-tips and the storage media during thermo-mechanical data bit formation process is a critical factor affecting the areal storage density, data bit writing/reading speed and system reliability. However, the phenomenon has yet been well understood. Molecular dynamics (MD) simulation is an ideal tool for addressing such an issue. Along with the experimental tests on the thermo-mechanical data bit formation process, MD simulation approach could provide useful information and in-depth understanding of the heat transfer phenomenon during the data writing process.

In this paper, the thermal properties of a nano-tip are analyzed using the nonequilibrium molecular dynamics (NEMD) simulation, which is a direct method that relies on imposing a temperature gradient and a heat flux across the system, and is therefore analogous to the experimental situation. In the NEMD simulation, the Tersoff-type *n*-body inter-atomic potential and the Gear's five-value predictor-corrector integration algorithm are employed to investigate the atomic movement in the nano-tip.

2 MODELING

2.1 Nano-Tip Structure

Single-crystal Si has a cubic lattice structure, known as the diamond lattice structure, characterized by strong directional bonding, low Poisson's ratio, strong temperature-sensitive yield strength and narrow dislocations with large Peierls-Nabarro forces. The atoms of silicon touch each other along the four <111> directions and the nearest-neighbour distance is $\sqrt{3}/4\, a_0$, where a_0 is the lattice constant (a_0=0.543 nm).

In this paper, a nano-tip with four-side pyramidal shape shown in Figure 1 is studied. Such a tip is convenient to construct using the anisotropic etching process technique. The inclined side face of the nano-tip is determined by a (111) plane in the Si crystal, well defined and yielding very sharp edges. The four adjacent diamond {111} planes form a 60^0 pyramidal crystal structure where the points of intersection of the planes constitute the vertices of the nano-tip. Therefore, the tip scans over the {100} planes that are parallel to the surface of the media substrate.

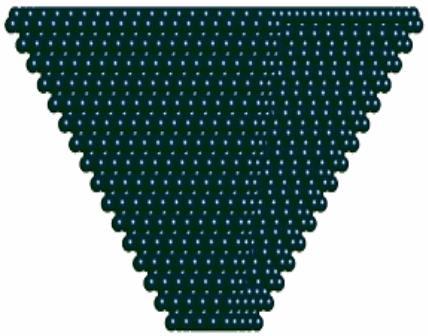

Figure 1 : Nano-tip pyramidal structure

In practice, a perfect 60^0 pyramid formed from a truncated diamond lattice is unstable at the atomic scale. The atoms on the {111} surfaces of the tip will reconstruct and the apex will evolve into certain curved surface. Furthermore, the tip blunts due to continuous operation and the curvature of the apex is modified with continuous use. Thus, in order to simulate the experimental situation, the first three unit cell layers of the tip apex in the {100} plane will be truncated in the tip model, as shown in Figure 1.

The Si atoms are arranged in 10 unit cell layers of the nano-tip. The height of the nano-tip is $10a_0$ = 5.43 nm, consisting of 10 Si (100) unit cell layers stacked upon each other. There are 7×7 atoms in the bottom surface of the tip, which corresponds to a contact area of approximate 5.31 nm^2 ($3\sqrt{2}a_0 \times 3\sqrt{2}a_0$), and there are 27×27 atoms in the top atom layer of the tip, which corresponds to a contact area of approximate 99.66 nm^2 ($13\sqrt{2}a_0 \times 13\sqrt{2}a_0$). The total number of atoms is 11890 in the tip model.

2.2 NEMD Simulation for Thermal Conductivity

In the NEMD simulation, the Gear's five-value predictor-corrector algorithm is used for the numerical integration of the equations of motion of individual atoms. The step time t is set at 0.57 *fs*, and the nano-tip is treated with fixed boundary condition.

The Tersoff-type n-body potential [5] is employed to describe the interactions between the silicon atoms in the nano-tip. The total Tersoff energy of the tip model is expressed in terms of the summation of atomic pair interactions, as a function of the atomic coordinates as follows:

$$V = \frac{1}{2}\sum_{i \neq j} W_{ij} \qquad W_{ij} = f_c(r_{ij})[f_R(r_{ij}) + b_{ij} f_A(r_{ij})] \tag{1}$$

$$f_R(r_{ij}) = A\exp(-\lambda r_{ij}) \quad f_A(r_{ij}) = -B\exp(-\mu r_{ij}) \tag{2}$$

$$f_c(r_{ij}) = \begin{cases} 1 & r_{ij} \le R \\ \frac{1}{2} + \frac{1}{2}\cos(\frac{r_{ij}-R}{S_{ij}-R_{ij}}\pi) & R \le r_{ij} \le S \\ 0 & r_{ij} \ge S \end{cases} \tag{3}$$

$$b_{ij} = \chi_{ij}(1+\beta_i^n \xi_{ij}^n)^{-1/2n} \qquad \xi_{ij} = \sum_{k \neq i,j} f_c(r_{ik}) g(\theta_{ijk})$$

$$g(\theta_{ijk}) = 1 + \frac{c^2}{d^2} - \frac{c^2}{d^2 + (h - \cos\theta_{ijk})^2} \tag{4}$$

where V is the system potential energy, W_{ij} is the bond energy for all the atomic bonds, i, j, k label the atoms, r_{ij} is the length of the ij bond, b_{ij} is the bond order term, θ_{ijk} is the bond angle between the bonds ij and ik, f_R represents a repulsive pair potential, f_A represents an attractive pair potential, f_C represents a smooth cutoff function to limit the range of the potential, and ζ_{ij} counts the number of other bonds to atom i besides the ij bond. The parameters A, B, R, S, λ, μ, β, n, c, d and h are constants which can be found in [5].

In order to investigate the thermal properties of the nano-tip, heat transformation is simulated with the NEMD and the thermal conductivity of the nano-tip is calculated based on the kinetics theory of gases and the Fourier's law[6] as follows.

$$k(T) = -\frac{J_z}{\nabla T_z} \tag{5}$$

where k is the thermal conductivity, $J_z(=\Delta\varepsilon/2At)$ is the heat flux vector defined as the amount of heat energy ($\Delta\varepsilon$) transferred per unit time (t) through unit area (A) perpendicular to the direction of the flux, and $\nabla T_z = \partial T/\partial z$ is the temperature gradient in the z direction along the tip height. Experimentally, k is typically obtained by measuring the temperature gradient based on a heat flux. In this simulation, it is calculated using the NEMD.

In the NEMD simulation, the system is divided into j slices along the z direction. The temperature of atoms in the slice is calculated in each iteration. The instantaneous temperature profile in each slice of the system centered at position z can be obtained by

$$T_j(t) = \left\langle \sum_{i=1}^{N_j} m_i v_i^2 \right\rangle \Big/ 3N_j k_B \tag{6}$$

where $T_j(t)$ is the temperature in the j_{th} slice, m_i and v_i are the mass and velocity of the i_{th} atom, < > denotes the statistical averaging over the entire simulation duration, N_j is the number of atoms in the i_{th} slice and k_B is the Boltzman constant.

The thickness of slice depends on the size of simulation system. According to the phonon mean free path (MFP) and the average phonon velocity [7], at least 30 atoms are needed in each slice to yield sufficient phonon-phonon scattering events within 1 *ns*. Furthermore, from the thermodynamic point of view, the temperature is a statistical parameter, which can be defined for any value of N_j at any time t. If the set of atoms is at the equilibrium temperature, T, the deviation of $T_j(t)$ will depend on T and the number of atoms: $|T_j(t)/T - 1| = 1/\sqrt{N_j}$ [8]. To obtain a good estimation of $T_j(t)$, N_j has to be adequately large so that $1/\sqrt{N_j}$ is smaller than the desired accuracy. Thus, we used at least 32 atoms in each slice.

The current NEMD simulation consists of two stages, the energy minimization process and the constant energy process. In the former stage, the system temperature keeps constant by rescaling the velocities of atoms in the system, and the potential energy minimization process is conducted on the system by relaxing the conformation. The energy

minimization is achieved if the instantaneous variations of the potential energy are less than 1 *meV*. After this process, the system will reach at the equilibrium status. To keep temperature constant, the velocity adjustment factor, α, is obtained by

$$\alpha^2 = \frac{3nk_B \cdot T_{obj}}{\sum_{i=0}^{n} m_i \cdot v_{i\_old}^2} \quad (7)$$

$$v_{i-new} = \alpha \cdot v_{i-old} \quad (8)$$

where n is the total number of atoms in the system, T_{obj} is the objective constant temperature, and v_{i_old} and v_{i_new} are the velocities of the i_{th} atom before and after rescaling, respectively.

The later stage is the constant energy process. A heat flux is imposed on the system along the z direction after equilibrium. It can be realized by keeping the temperatures of the hot (T_{hot}) and cold (T_{cold}) thermal reservoirs constant and setting T_{hot} - T_{cold} = *150K* in this simulation. These two temperatures can be obtained from Eqs.(7) and (8). The hot and cold thermal reservoirs are located at the top and bottom ends of the nano-tip, respectively. During the simulation, the kinetic energies added to the hot thermal reservoir ($\Delta\varepsilon_{hot}$) and removed from the cold thermal reservoir ($\Delta\varepsilon_{cold}$) are calculated. Thus, the heat flux can be obtained from

$$J_z = \frac{\Delta\varepsilon_{hot} + \Delta\varepsilon_{cold}}{2A(z) \cdot t} \quad (9)$$

3 RESULTS AND DISCUSSION

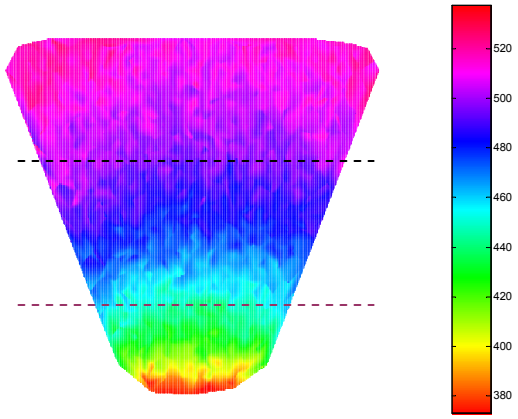

Figure 2 : Temperature distribution in the nano-tip

Figure 2 shows a contour plot of the temperature distribution in the nano-tip. It can be found that at the same high level (as shown in Figure 2 by dash lines), the temperature of the region near the boundary is a bit higher than that far from the boundary, which is resulted from the fixed boundary conditions. This phenomenon indicates that there exists substantial reflection of phonons and phonon boundary-scattering at the boundary.

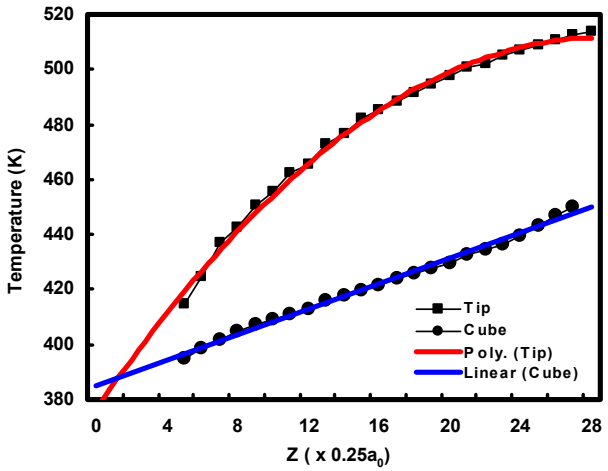

Figure 3 : Temperature profiles of nano-tip and nano-cube, represented by full squares and full circles respectively. The red line is the polynomial fitting of the nano-tip temperature profile and the blue line is the least-square linear fitting of the nano-cube temperature profile.

Figure 3 shows the temperature profile of the nano-tip model in the z direction. Since the cross sectional areas of the tip are not constant, in order to compare with the conventional nano-structure configurations, a silicon nano-cube ($10a_0 \times 10a_0 \times 10a_0$) is also simulated with the same simulation conditions as the nano-tip. The temperature profile of the nano-cube is also shown in Figure 3. As expected, it is observed that the temperature of the nano-cube is linearly distributed, and thus, the temperature gradient is constant ($\nabla T_z = 1.7 \times 10^{10} K \cdot m^{-1}$ in this case) because of the constant cross sectional area. The thermal conductivity of the nano-cube can be calculated based on the Fourier's law as k~2.7W/mk. In contrast, because of the varying cross sectional area, the temperature of the nano-tip is nonlinearly distributed, and the temperature gradient is therefore non-constant. The integral mean of the thermal conductivity of the nano-tip can be obtained as $\overline{k}$ ~1.1W/mk. Furthermore, it can be found that with the increase of the cross sectional area along the z direction, the temperature gradient decreases homologously, which indicates that the finite size and structural configuration effects on thermal transport weaken with the increasing system size.

4 SUMMARY

The thermal properties of nano-tip have been investigated by NEMD simulation. Obvious structural

configuration and boundary condition effects on the thermal transport have been observed due to the phonon boundary-scattering and possible phonon spectrum modification. Moreover, the thermal conductivity of the nano-tip has been calculated. The results provide some insights for the future design optimization of the nano-tip structures. This study also builds up the foundation for the study of heat transfer between the nano-tips and the media during thermo-mechanical data bit formation process in the thermal-assisted data storage technologies.

REFERENCES

[1] Robert E. Rottmayer, Sharat Batra, Dorothea Buechel, William A. Challener, Julius Hohlfeld, Yukiko Kubota, Lei Li, Bin Lu, Christophe Mihalecea, Keith Mountfield, Kalman Pelhos, Chubing Peng, Tim Rausch, Michael A. Seigler, Dieter Weller, and XiaoMin Yang, "Heat-Assisted Magnetic Recording", IEEE Transactions on Magnetics, Vol. 42, No. 10, pp. 2417-2421, 2006

[2] P. Vettiger, G. Cross, M. Despont, U. Drechsler, U. Durig, B. Gotsmann, W. Haberle, M. A. Lantz, H. E. Rothuizen, R. Stutz, and G. K. Bing, "The "Millipede" – Nanotechnology Entering Data Storage, " IEEE Transactions on Nanotechnology, Vol. 1, No. 1, pp. 39-55, 2002

[3] G. Binning, M. Despont, U. Drechsier, W. Haberle, M. Lutwyche, P. Vettiger, H. J. Mamin, B. W. Chui, and T. W. Kenny, "Ultrahigh-Density Atomic Force Microscopy Data Storage with Erase Capability," Applied Physics Letters, Vol. 76, pp. 1329-1331, 1999

[4] S. Gidon, O. Lemonnier, B. Rolland, O. Bichet, C. Dressler, and Y. Samson, "Electrical Probe Storage using Joule Heating in Phase Change Media," Applied Physics Letters, Vol. 85, No. 26, pp. 6392-6394, 2004

[5] J. Tersoff, "Modeling Solid-state Chemistry: Interatomic Potentials for Multicomponent Systems," Physical Review B, Vol. 39, No. 8, pp. 5566 (1989)

[6] Charles Kittel, "Introduction to Solid State Physics, " Eighth Edition, New York, pp. 90, 2005

[7] A. Maiti, G. D. Mahan and S. T. Pantelides, "Dynamical Simulations of Nonequilibrium Processes – Heat Flow and the Kapitza Resistance Across Grain Boundaries," Solid State Communications, Vol. 102, No. 7, pp. 517-521, 1997

[8] B. Diu, C. Guthmann, D. Lederer, and B. Roulet, Elements de Physique Statistique, Paris: Hermann, pp. 1002, 1989